4-23-2018

Rapid Assessment of the Ce-Co-Fe-Cu System for Permanent Magnetic Applications

Fanqiang Meng
Ames Laboratory, mengfq@ameslab.gov

Rakesh P. Chaudhary
Ames Laboratory, rakeshc@ameslab.gov

Kinjal Gandha
Ames Laboratory, kgandha@ameslab.gov

I. C. Nlebedim
Ames Laboratory, nlebedim@ameslab.gov

Andriy Palasyuk
Ames Laboratory, palasyuk@ameslab.gov

See next page for additional authors

Rapid Assessment of the Ce-Co-Fe-Cu System for Permanent Magnetic Applications

Abstract
This work focuses on the rapid synthesis and characterization of quaternary Ce(CoFeCu)5 alloy libraries to assess their potential viability as permanent magnets. Arrays of bulk specimens with controlled compositions were synthesized via laser engineered net shaping (LENS) by feeding different ratios of alloy powders into a melt pool created by a laser. Based on the assessment of the magnetic properties of the LENS printed samples, arc-melted and cast ingots were prepared with varying Fe (5–20 at.%) and Co (60–45 at.%) compositions while maintaining constant Ce (16 at.%) and Cu (19 at.%) content. The evolution of the microstructure and phases with varying chemical compositions and their dependence on magnetic properties are analyzed in as-cast and heat-treated samples. In both the LENS printed and cast samples, we find the best magnetic properties correspond to a predominantly single-phase Ce(CoFeCu)5 microstructure in which high coercivity (Hc > 10 kOe) can be achieved without any microstructural refinement.

Disciplines
Materials Science and Engineering | Metallurgy

Authors
Fanqiang Meng, Rakesh P. Chaudhary, Kinjal Gandha, I. C. Nlebedim, Andriy Palasyuk, Emrah Simsek, Matthew J. Kramer, and Ryan T. Ott

Rapid assessment of Ce-Co-Fe-Cu system for permanent magnetic applications

F. Meng, [1,2,*] R. P. Chaudhary, [1,*] K. Gandha, [1] I. C. Nlebedim, [1] A. Palasyuk, [2] E. Simsek, [1] M. J. Kramer, [1,2] R. T. Ott[1,2]

1-The Critical Materials Institute, Ames Laboratory (USDOE), Ames, IA 50011, USA

2-Division of Materials Science and Engineering, Ames Laboratory (USDOE), Ames, IA 50011, USA

*mengfq@ameslab.gov

*rakeshchaudhary@ameslab.gov

This work focuses on rapid synthesis and characterization of quaternary $Ce(CoFeCu)_5$ alloy libraries to assess their potential viability as permanent magnets. Arrays of bulk specimen with controlled compositions were synthesized via Laser Engineered Net Shaping (LENS) by feeding different ratios of alloy powders into a melt pool created by a laser. Based on the assessment of the magnetic properties of the LENS printed samples, arc-melted and cast-ingots were prepared with varying Fe (5-20 at.%) and Co (60-45 at.%) compositions, while maintaining constant Ce (16 at.%) and Cu (19 at.%) content. The evolution of microstructure and phases with varying chemical compositions and their dependence on magnetic properties are analyzed in as-cast and heat treated samples. In both the LENS printed and cast samples, we find the best magnetic properties correspond to a predominantly single phase, $Ce(CoFeCu)_5$, microstructure in which high coercivity (H_c > 10 kOe) can be achieved without any microstructural refinement.

INTRODUCTION

High-performance permanent magnets with enhanced energy product and thermal stability requires critical and expensive materials such as Nd, Sm, Dy and Co.[1-3] Supply challenges and price instability associated with these elements, however, have prompted the need to develop viable alternative magnet alloys with reduced critical elements.[4-8] Conventional permanent magnet synthesis typically involves complex multi-step processing[9], which can be a rate limiting step in new alloy development. Developing new, or improvement in existing permanent magnet alloys with decreased amounts of critical materials requires accelerating both the alloy synthesis and property characterization. This will enable rapid screening of large ranges of compositions and microstructural phase space and identification of trends in structure-property relationships. Combinatorial synthesis via thin film or additive manufacturing coupled with high-throughput characterization methodologies is an attractive approach for developing new magnetic materials, however, this has been mostly limited to soft magnetic materials.[10-17]

In this work, we used bulk combinatorial synthesis via 3D metal printing, i.e., Laser Engineered Net Shaping (LENS), coupled with high-throughput characterization techniques to rapidly identify potential permanent magnet alloy compositions in the Ce-Co-Fe-Cu quaternary system. The Ce-Co-Fe-Cu system was chosen based on recent work by Palasyuk et al. which has shown that high coercivity can be obtained in single crystals of 1:5 Ce-Co-Cu and 1:5 Ce-Co-Fe-Cu without any microstructural refinement.[18]

The magnetic properties as a function of alloy composition have been evaluated to assess the trends in structure-property relationship for the library and identify the best

candidate(s) composition for optimization using traditional casting methods. Arc-melted and cast-ingots were prepared based on the identified candidates from the rapid assessment study. The microstructural evolution, phase formation, and magnetic properties of the cast alloys are investigated and discussed.

EXPERIMENTAL

A library of alloys was synthesized by 3D printing using an Optomec MR-7 LENS system. A melt pool was created on a stainless steel substrate by the Ytterbium laser (wavelength of 1070 nm, power of 100 W) into which three different pre-alloyed powders were fed at a pre-determined rate. The pre-alloyed powders were obtained by crushing/grinding and sieving ingots of $CeCo_5$, $Ce(Co_{0.5}Cu_{0.5})_5$, and Ce_2Fe_{17} purchased from ACI Alloys Inc. to obtain powders in the size range of 45 to 150 microns. During melting, the print head was drawn upward at a rate of 0.2 mm/s (no rastering in x- or y-directions) to form rods of diameter, $D \approx 3$ mm and height $H \approx 20$ mm. All the LENS samples (25) were printed in 2 hours, compared to conventional process that may take days or weeks to prepare equivalent number of samples.

The morphology of as-printed rod-shaped samples are shown in Figure 1a. To promote compositional uniformity the as-printed rods were wrapped in Tantalum foil and sealed in quartz tube in Ar atmosphere and then heat treated at 900 ^oC for 96 h followed by aging at 400 ^oC for 24 h followed by furnace cooling to room temperature.

The arc melted and drop-casted bulk specimens with diameter of 10 mm were prepared by the Materials Preparation Center at Ames Laboratory using 99.9% pure cerium and cobalt, and 99.99% pure iron, and copper.[19] Identical heat treatment

procedures were used on the cast samples as on the LENS printed samples to optimize the microstructure.

The chemical compositions of the as-printed and as-cast samples along with the heat treated samples were measured by x-ray fluorescence (XRF) using a Bruker M4 TORNADO Micro-XRF spectrometer (μ-XRF; 25 μm spot size) operated at 50 kV and 300 μA (Rh target). Magnetic properties were measured up to 30 kOe using a Quantum Design vibrating sample magnetometer (VSM). The Curie temperatures (Tc) were measured by performing thermogravimetric analysis (TGA) in magnetic field using an NETZSCH STA 449 F3 Jupiter thermal analyzer with auto sampler, as described in Ref. 17. Structural characterization was performed using a FEI Teneo field emission scanning electron microscope (SEM) equipped with Oxford Energy dispersive X-ray spectroscopy (EDS).

RESULTS AND DISCUSSION

The chemical compositions of the LENS printed samples measured using μ-XRF (after heat treatment) are shown in the pseudo-ternary Ce-Co-FeCu diagram in Fig. 1b. For the 25 different samples that were prepared, a large range of composition with varying amount of Ce, Co, Fe and Cu is observed. The goal of this study was to straddle the compositions around the 1:5 Ce-Co composition, while substituting different amounts of Cu and Fe for Co. Binary $CeCo_5$ is a hexagonal intermetallic compound with a single easy axis, large magnetocrystalline anisotropy at room temperature ($K_1 = 7.2 \times 10^7$ erg/cm^3), and moderate saturation magnetization 4π Ms = 8700 Gauss (81 emu/g for ρ = 8.54 emu/g).[20] Moreover, it has a very high anisotropy field, H_A = 200 kOe, with a theoretical upper limit for energy product of 18.9 MGOe.[20] These properties make this

compound an attractive permanent magnet since Ce, while a rare earth, is in abundance. However, decreasing the critical element Co is also important. Past work has shown that substitutions of Fe and Cu can have a beneficial effect on some of the permanent magnetic properties of the $CeCo_5$ system and thus are ideal alloying additions for this combinatorial study.[21]

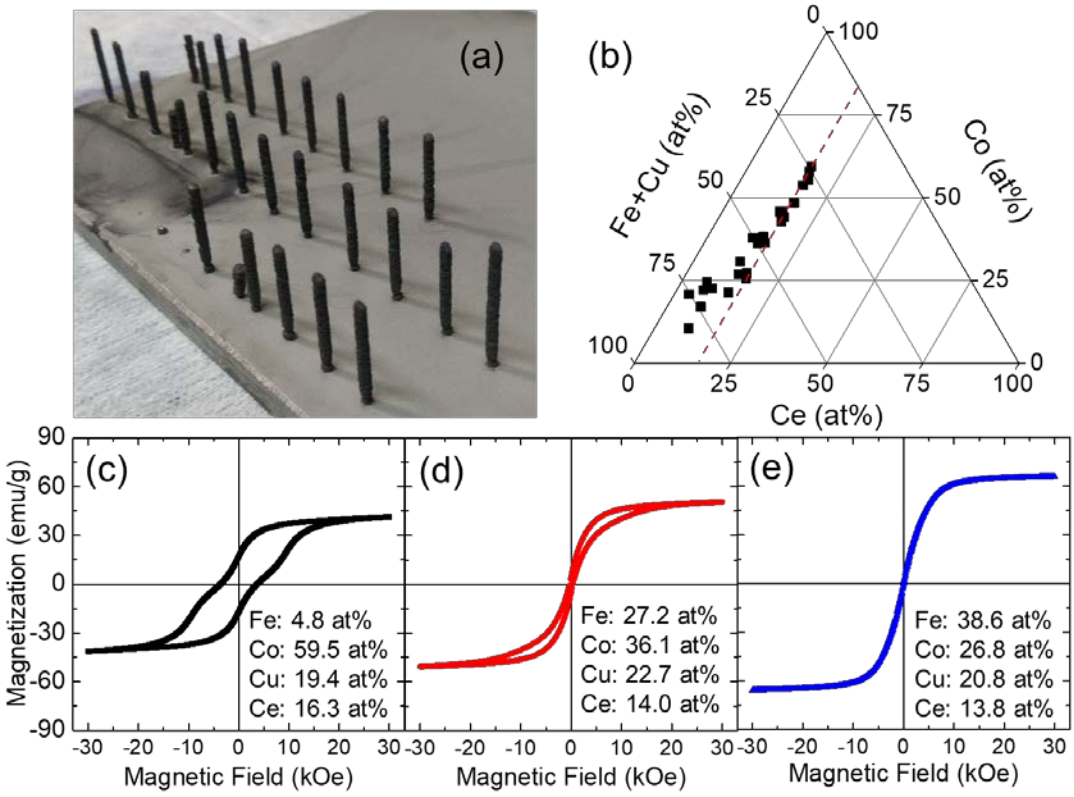

Fig. 1 (a) As-printed bulk Ce-Co-Fe-Cu rods on stainless steel substrate, (b) chemical composition distribution in ternary Ce -Co- FeCu diagram, and (c-e) magnetic hysteresis loops measured by VSM of the LENS printed rods with different chemical compositions.

Fig. 1c-1e shows representative magnetic hysteresis loops of the printed rods after heat-treatment with different chemical compositions as shown in inset. The results show quite clearly that the hard magnetic properties decreased with Fe content for the LENS

printed samples. As mentioned above, LENS printing has primarily been used for synthesizing soft magnetic materials, [10-12, 17] therefore it is interesting that the process can be used to identify potential permanent magnet materials, even in complex materials systems.

Fig. 2a and 2b shows the contour plots of coercivity (Hc) and saturation magnetization (Ms) respectively, extracted from hysteresis loops of the LENS samples as a function of Ce-Co-FeCu composition. Furthermore, the lowest Curie temperature (Tc) of the samples are shown in Fig. 2c. From the contour plots, it can be seen that Hc increases with increasing Co content (Fig. 2a) which indicates that Co plays stronger role in enhancing magnetocrystalline anisotropy than Fe. The Ms increases with increasing Fe content (Fig. 2b) in line with the fact that the magnetic moment per atom for Fe (2.2 Bohr magnetons) is higher than that for Co (1.7 Bohr magnetons). Moreover, the Tc varies as a function of Fe, Cu and Co (Fig. 2c). This competing property-composition dependencies highlights the difficulties in identifying optimal alloy compositions for permanent magnet alloy applications and the need for accelerated alloy development. For example, certain compositions show good Hc, but poor Ms and/or Tc while the opposite is true for other compositions, which might exhibit high Ms, but low Hc and Tc. To help identify compositions that will potentially achieve a good combination of properties for permanent magnet applications, we normalized all the measured data to some minimum properties (Hc = 2 kOe, Ms = 40 emu/g and Tc = 400 °C) and then plotted the compositions that met these minimum requirement on the radar plot shown in Fig. 2d. It is important to note that Tc and Ms are intrinsic properties, which are not likely to change much with microstructural optimization, while Hc is an extrinsic property that can be

highly dependent on microstructure. Therefore, it is difficult to down select the compositions based on Hc, since we cannot be certain what values could be realized with additional processing. Regardless, we based our down select criteria on the best combination of Tc, Ms and Hc in the heat-treated LENS samples and identified the approximate composition of $Ce_{16.3}Co_{59.5}Fe_{4.8}Cu_{19.4}$ at.%. Using conventional arc melting and drop casting we synthesized this composition along with 3 other alloys with different amounts of Fe and Co as shown in Table 1, based on the formula $CeCo_{5-x-y}Cu_xFe_y$.

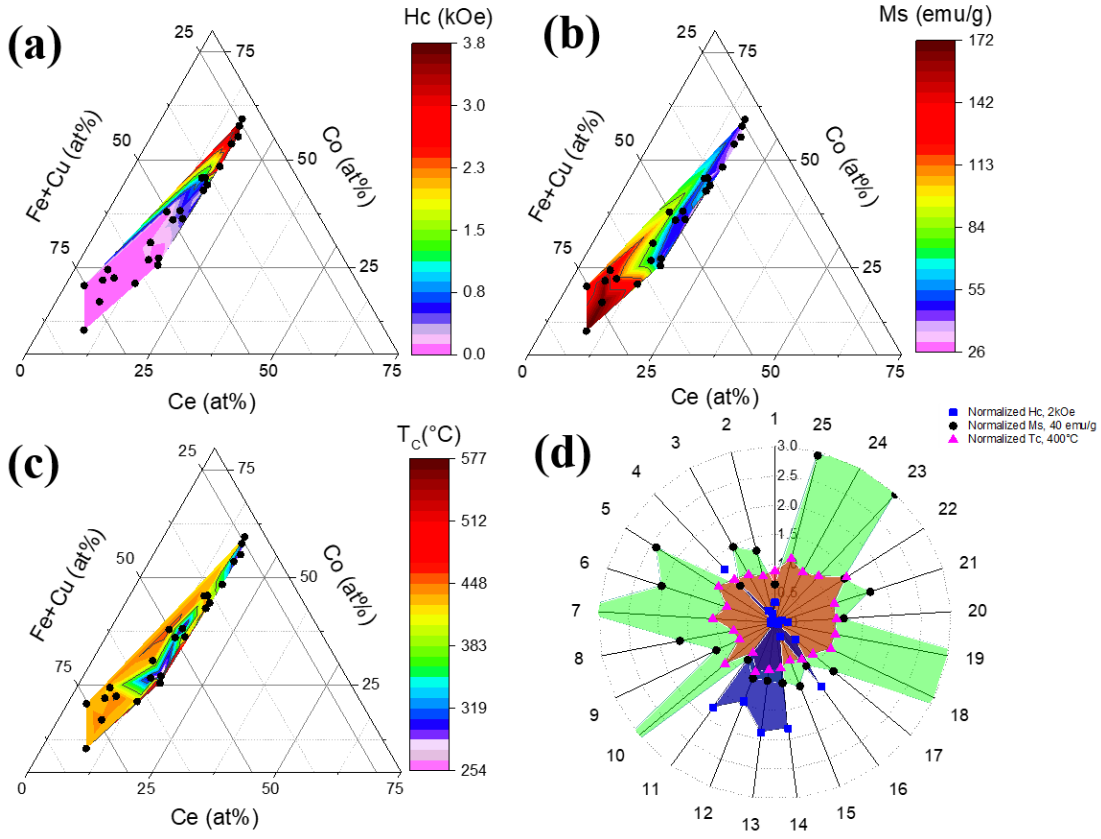

Fig. 2 Contour plots of magnetic properties (a) coercivity (Hc), (b) saturation magnetization (Ms), and (c) Curie temperature (Tc) as a function of the Ce-Co-FeCu compositions extracted from hysteresis loops. Fig. 2d Radar plot of LENS printed samples after heat treatment with different composition with normalized Hc, Ms, and Tc.

Fig. 3 shows the magnetic hysteresis loops of as-cast and heat-treated samples of composition $Ce_{16.3}Cu_{19.4}Co_{59.5-x}Fe_x$. The values of Hc and Ms are summarized in the Table 1. Similar to LENS printed sample, as cast and heat treated 5 at.% Fe sample show a significant Hc, with values over 10 kOe for heat treated sample. It can also be seen from Fig.1c and 3a that the LENS printed sample and arc-melted samples with 5 at.% Fe exhibit canted magnetic hysteresis loops. This type of hysteresis loop is typical of non-coherent switching involving either of the following: decoupled hard and soft magnetic phases, large and small grains, compositional variations or a combination of those. It is more likely to arrive at any of those conditions that lead to non-coherent switching in LENS printed samples, compared to arc-melted samples. For example, arc–melted samples are prepared by melting stoichiometric amounts of Ce and Co (99.9%) and Fe and Cu (99.99%) on a water-cooled copper mold. The ingots were turned over and remelted several times for homogenization. On the other hand, LENS printed samples were prepared by feeding three different pre-alloyed powders of $CeCo_5$, $Ce(Co_{0.5}Cu_{0.5})_5$, and Ce_2Fe_{17}. During melting, the print head was drawn upward to form rods. Therefore, the surface layer of the printed rod potentially contains partially melted powders and/or inhomogeneous mixing. Compared with arc-melted samples, solidification in LENS printed samples is more rapid and often leads to metastable phase formation. It is possible that the printed samples, even after heat treatment, still retained some inhomogeneity leading to soft or hard phases that are responsible for two-phase hysteresis loop.

With increasing Fe content up to 15 at.%, Hc slightly increases in the as-cast samples and then shows a precipitous drop for as cast sample containing 20 at.% Fe. Hc

decreases monotonically (10.8 to 5.4 kOe) with increasing Fe content for heat treated sample. It can also be seen from the magnetic hysteresis loops in Fig. 3 that the magnetization does not saturate. The anisotropy field of $CeCo_5$ is significantly higher, ~200 kOe. Alloying additions of Fe and Cu for Co appears to increase the anisotropy field, which can be the primary reason for the magnetization not to saturate. Increasing the Fe to 15 at.% results in a homogenous microstructure of $Ce(CoFeCu)_5$ as the primary phase with high Hc. Further increase in Fe to 20 at.% results in an increase in Ms, but a decrease in Hc. From the hysteresis loops, it is clear that the heat treatment of cast alloys leads to a significant increase in Hc relative to the as-cast state. The heat treated cast rods show a maximum BH_{max} of 3 MGOe for 10 at.% Fe. While the magnetic properties are not comparable to $SmCo_5$ magnet alloys, the relative decrease in Co along with the improved processing flexibility makes the identified compositions potentially interesting for permanent magnet applications. Furthermore, the alignment of crushed powder can enhance the magnetic properties via microstructural refinement, and such, will be the focus of future work.

Table 1. Summary showing coercivity (Hc), remanence magnetization (Mr) and magnetization (M at 30kOe) values from hysteresis loop with varying composition before (As-cast) and after heat treatment (HT).

Sample	Composition (at.%)				Hc(kOe)	M@30kOe (emu/g)	Mr(emu/g)	Hc(kOe)	M@30kOe (emu/g)	Mr(emu/g)
	Ce	Co	Fe	Cu	As-cast	As-cast	As-cast	HT	HT	HT
5Fe	16.3	59.5	4.9	19.4	2.2	32.9	21.2	10.8	31.9	23.5
10Fe	16.3	54.5	9.9	19.4	2.6	43.1	31	9	43.7	35.9
15Fe	16.3	49.5	14.9	19.4	2.5	42.8	18	8.7	42.1	28.4
20Fe	16.3	44.5	19.9	19.4	0.8	52.3	15.3	5.4	57.5	24

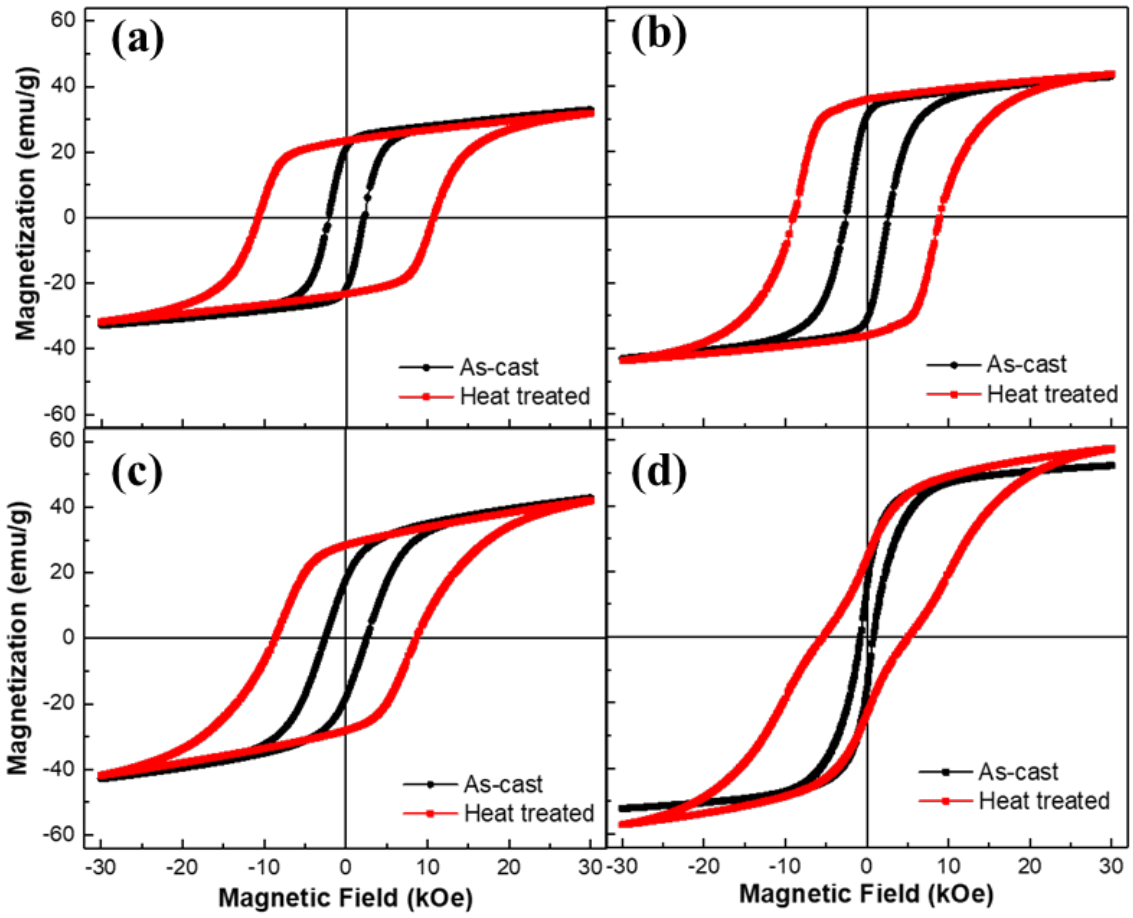

Fig. 3 Magnetic hysteresis loop of as-cast and heat treated $Ce_{16.3}Cu_{19.4}Co_{59.5-x}Fe_x$ samples where x = (a) 5 at.% Fe, (b) 10 at.% Fe, (c) 15 at.% Fe and (d) 20 at.% Fe.

To better understand the mechanisms behind the increase in Hc after heat treatment, the microstructure of the as-cast and heat treated alloys with varying Fe content were examined using back-scattered SEM, Fig. 4. It is known that $CeCo_5$ has hexagonal $CaCu_5$ structure,[22] while Ce_2Co_7 and Ce_2Co_{17} may exist in either hexagonal or rhombohedral modifications, which are simply derivable from the basic $CaCu_5$ packing. The close structural relationship between the 2:7, 1:5, and 2:17 phases can lead to some mutual solubility at high temperatures, particularly with Cu and Fe alloying

additions.[23] EDS measurements of as-cast samples with 5 at.% Fe (Fig. 4a) shows mainly $Ce(CoFeCu)_5$ and a small amount of $Ce_2(CoFeCu)_7$ phase, which exhibit brighter contrast as marked by arrow. Looking at Figs. 4(c), (e) and (g), we see that with increasing Fe concentration, the volume fraction of secondary phases [$Ce_2(CoFeCu)_7$ and $Ce_2(CoFeCu)_{17}$] increases, which is confirmed by EDS measurements shown in Table 2. Based on image analysis, for 5 at.% Fe sample, the volume fraction of $Ce_2(CoFeCu)_7$ (region A) is ~1.5%, which increases to ~6.3% in the 10 at.% Fe sample as indicated by more clear and brighter white phase in Fig. 4c. Additionally, a few bands of darker grey contrast (region C) are embedded in the gray matrix of $Ce(CoFeCu)_5$ phase (region B), which approximately corresponds to $Ce(CoFeCu)_5$ composition, but deviate from the matrix. EDS mapping of light and dark bands of 10 at.% Fe (Fig. 5) reveals that dark regions are rich in Co and Fe, and poor in Cu and Ce. Moreover, brighter phases are rich in Ce. EDS measurements indicates that bright phase is from $Ce_2(CoFeCu)_7$, light grey region of the matrix is $Ce(CoFeCu)_5$ and dark region is poor in Ce with slight deviation in composition from $Ce(CoFeCu)_5$ phase.

Table 2. EDS point measurements from different region in the as-casted samples with 10 and 15 at.% Fe

As-cast, 10 at% Fe					**As-cast, 10 at% Fe**				
Region	**Ce**	**Co**	**Cu**	**Fe**	**Region**	**Ce**	**Co**	**Cu**	**Fe**
A-$Ce_2(CoFeCu)_7$	22.0	52.1	18.6	7.3	D-Fe(Co)	0.7	60.1	4.2	35.0
B-$Ce(CoCuFe)_5$	16.0	47.5	28.4	8.1	E-$Ce(CoCuFe)_5$	15.9	52.3	18.1	13.7
C-$Ce(CoCuFe)_5$	14.0	58.5	15.3	12.2	F-$Ce_2(CoCuFe)_7$	21.0	51.1	17.6	10.3

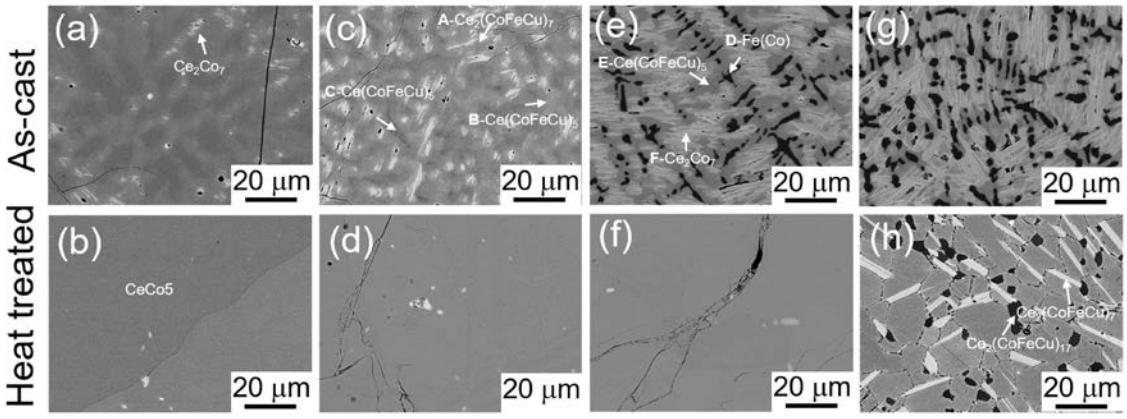

Fig. 4 Back-scatted SEM images of as-cast (upper row) and heat treated (lower row) samples of composition $Ce_{16.3}Cu_{19.4}Co_{59.5-x}Fe_x$ with varying x; where x = (a), (b) 5 at.% Fe, (c), (d) 10 at.% Fe, (e), (f) 15 at.% Fe and (g), (h) 20 at.% Fe

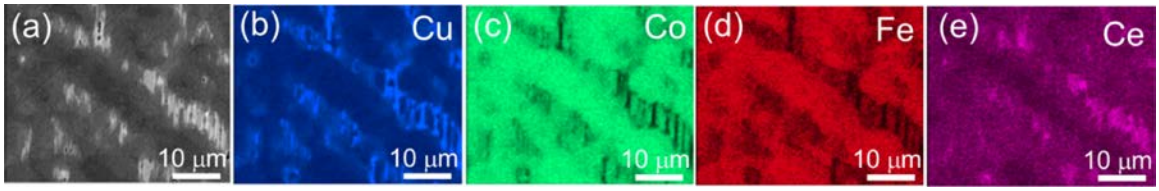

Fig. 5(a) Back-scatted SEM image of as-cast sample with 10 at.% Fe and corresponding EDS mapping (b) Cu, (c) Co, (d) Fe and (e) Ce.

Addition of Fe up to 15 at.% and 20 at.% results in the formation of dark dendrites in as cast samples shown in Fig. 4(e) and Fig. 4(g). EDS analysis shows that the dendrites are enriched with Fe and Co (region D) and surrounded by the $Ce(CoFeCu)_5$ phase in matrix. The $Ce_2(CoFeCu)_7$ phase exhibits a lamellar morphology and is brighter than other phases. Based on image analysis, volume fraction of both $Ce_2(CoFeCu)_7$ and

Fe(Co) phases appear to increase with increasing Fe content from 15 to 20 at.% Fe, while $Ce(CoFeCu)_5$ phase fraction decreases.

The microstructures developed after heat treatment for 5, 10 and 15 at.% Fe are shown in Fig. 4 (b), (d) and (f), respectively. It is noteworthy that microstructures of 5-15 at.% Fe samples appear to become much more homogenized by the heat treatment, with chemical analysis showing primarily $Ce(CoFeCu)_5$ phase. The nature of the small amount of bright phase embedded in $Ce(CoFeCu)_5$ matrix is unclear, and is part of continued investigation.

It is well known that Hc is a structure sensitive extrinsic property affected by any structure change (e.g., morphology).[24] Therefore, it is unusual to observe high values of Hc in samples with large grains (~100 – 300 μm) and no obvious precipitates that may serve as a domain pinning sites. Thus, since 5-15 at.% Fe heat-treated samples result in formation of only $Ce(CoFeCu)_5$ phase with hexagonal crystal structure, the observed high Hc may be attributed to very high uniaxial anisotropy of this compound. This intrinsic magnetic subtleties will be clarified in the subsequent work. In contrast, the microstructure of heat-treated sample with 20 at.% Fe shows precipitate of $Ce_2(CoFeCu)_{17}$ phase at grain boundaries. The rectilinear grains of $Ce_2(CoFeCu)_7$ phase are embedded inside the grains. The chemical composition of the matrix is still $Ce(CoFeCu)_5$, however there is a significant amount of 2-17 and 2-7 phases, which change the anisotropy, but appear to decrease Hc with this composition and/or grain size. This leads to a trade-off, i.e., decrease in Hc and increase in Ms. The 1:5 phase with a single easy axis, large magnetocrystalline anisotropy and very high anisotropy field is very important to the development of high Hc in this system.

CONCLUSION

We have used bulk combinatorial synthesis via LENS coupled with high-throughput characterization techniques, to rapidly assess Ce-Co-Fe-Cu alloys with decreased critical elements for permanent magnet applications. Bulk sample libraries synthesized by LENS proved ideal for high-throughput characterization techniques of magnetic, thermal and structural properties. Using this approach, we have rapidly identified promising compositions and prepared those by more conventional melt processing and casting synthesis. The arc melted and cast alloys exhibited the predicted good combination of magnetic properties after heat treatment including high Hc (> 10 kOe), which validates the robustness of using this rapid assessment approach to accelerate magnet alloy development.

ACKNOWLEDGEMENTS

This work is supported by the Critical Materials Institute, an Energy Innovation Hub funded by the U.S. Department of Energy, Office of Energy Efficiency and Renewable Energy, Advanced Manufacturing Office. The Ames Laboratory is operated by Iowa State University under Contract No. DE-AC02-07CH11358. We are also appreciative to Sergey L. Bud'ko and Paul C. Canfield for valuable inputs and recommendations.

REFERENCES

1 K. Gandha, K. Elkins, N. Poudyal, X. Liu, J. P. Liu, *Scientific Reports* **2014**, *4*, 5345 10.1038/srep05345.

2 O. Gutfleisch, M. A. Willard, E. Brück, C. H. Chen, S. G. Sankar, J. P. Liu, *Advanced Materials* **2011**, *23*, 821-842 10.1002/adma.201002180.

3 J. M. D. Coey, *IEEE Transactions on Magnetics* **2011**, *47*, 4671-4681 10.1109/TMAG.2011.2166975.

4 M. J. Kramer, R. W. McCallum, I. A. Anderson, S. Constantinides, *JOM* **2012**, *64*, 752-763 10.1007/s11837-012-0351-z.

5 R. Skomski, P. Manchanda, P. Kumar, B. Balamurugan, A. Kashyap, D. J. Sellmyer, *IEEE Transactions on Magnetics* **2013**, *49*, 3215-3220 10.1109/TMAG.2013.2248139.

6 E. A. Nesbitt, G. Y. Chin, P. K. Gallagher, R. C. Sherwood, J. H. Wernick, *Journal of Applied Physics* **1971**, *42*, 1530-1532 10.1063/1.1660325.

7 E. A. Nesbitt, *Journal of Applied Physics* **1969**, *40*, 1259-1265 10.1063/1.1657619.

8 R. C. Sherwood, E. A. Nesbitt, G. Y. Chin, M. L. Green, *Materials Research Bulletin* **1972**, *7*, 489-493 https://doi.org/10.1016/0025-5408(72)90151-1.

9 K. Kumar, *Journal of Applied Physics* **1988**, *63*, R13-R57 10.1063/1.341084.

10 C. V. Mikler, V. Chaudhary, T. Borkar, V. Soni, D. Jaeger, X. Chen, R. Contieri, R. V. Ramanujan, R. Banerjee, *JOM* **2017**, *69*, 532-543 10.1007/s11837-017-2257-2.

11 T. Borkar, R. Conteri, X. Chen, R. V. Ramanujan, R. Banerjee, *Materials and Manufacturing Processes* **2017**, *32*, 1581-1587 10.1080/10426914.2016.1244849.

12 B. Zhang, N.-E. Fenineche, H. Liao, C. Coddet, *Journal of Magnetism and Magnetic Materials* **2013**, *336*, 49-54 https://doi.org/10.1016/j.jmmm.2013.02.014.

13 E. M. H. White, A. G. Kassen, E. Simsek, W. Tang, R. T. Ott, I. E. Anderson, *IEEE Transactions on Magnetics* **2017**, *53*, 1-6 10.1109/TMAG.2017.2711965.

14 M. L. Green, I. Takeuchi, J. R. Hattrick-Simpers, *Journal of Applied Physics* **2013**, *113*, 231101 10.1063/1.4803530.

15 K. Rajan, *Annual Review of Materials Research* **2008**, *38*, 299-322 10.1146/annurev.matsci.38.060407.130217.

16 S. I. Woo, K. W. Kim, H. Y. Cho, K. S. Oh, M. K. Jeon, N. H. Tarte, T. S. Kim, A. Mahmood, *QSAR & Combinatorial Science* **2005**, *24*, 138-154 10.1002/qsar.200420061.

17 J. Geng, I. C. Nlebedim, M. F. Besser, E. Simsek, R. T. Ott, *JOM* **2016**, *68*, 1972-1977 10.1007/s11837-016-1918-x.

18 A. P. et.al., *62nd Annual Conferences on Magnetism and Magnetic Materials* **2017**, 632.

19 USDOE-BES. Materials Preparation Center at Ames Laboratory, Ames, IA, USA. Available from:<www.mpc.ameslab.gov>.

20 K. Strnat, G. Hoffer, J. Olson, W. Ostertag, J. J. Becker, *Journal of Applied Physics* **1967**, *38*, 1001-1002 10.1063/1.1709459.

21 E. A. Nesbitt, G. Y. Chin, R. C. Sherwood, J. H. Wernick, *Applied Physics Letters* **1970**, *16*, 312-313 10.1063/1.1653207.

22 T. Yoshio, S. Harufumi, *Japanese Journal of Applied Physics* **1968**, *7*, 966.

23 H. Leamy, M. Green, *IEEE Transactions on Magnetics* **1973**, *9*, 205-209 10.1109/TMAG.1973.1067642.

24 R. Skomski, D. J. Sellmyer, in *Handbook of Advanced Magnetic Materials*, ed. by Y. Liu, D. J. Sellmyer, D. Shindo, Springer US, Boston, MA, **2006**, pp. 1-57.